Soil Dynamics and Earthquake Engineering 114 (2018) 242–252

Contents lists available at ScienceDirect

Soil Dynamics and Earthquake Engineering

journal homepage: www.elsevier.com/locate/soildyn

Effect of soil structure interaction on the dynamic responses of base isolated bridges and comparison to experimental results

Wentao Dai[a,*], Fabian Rojas[b], Chen Shi[c], Yong Tan[d]

[a] Dalian Maritime University, Dalian 116000, China
[b] University of Chile, Blanco Encalada 2002, Santiago, Chile
[c] College of Petroleum Engineering, China University of Petroleum, Qingdao 266580, China
[d] Department of Geotechnical Engineering, Tongji University, Shanghai 200092, China

ARTICLE INFO

Keywords:
Soil structure interaction
Base isolation
Pile foundation
Frequency domain
Continuous mass distribution
Transfer functions

ABSTRACT

In this paper, the effect of soil structure interaction and base isolation on the dynamic characteristics of an instrumented bridge is examined using transfer functions and measured motions in the frequency domain. A three dimensional structural model in the frequency domain which accounts for continuous mass distribution along each member and the effect of axial forces as well as rotary inertia is adopted. The dynamic stiffness of pile foundations and surface mat foundation underneath piers, determined separately using appropriate numerical methods, is incorporated into the structural model and the global stiffness matrix. Results are obtained for models of a bridge both without and with isolation pads for various values of the equivalent shear stiffness. This allows one comparing the values of the predominant frequencies and the dynamic amplification of the motions over the frequency range of interests. The transfer functions are also obtained at the bottom of the piers to evaluate the impact and importance of soil structure interaction effect on the dynamic behavior of the system. Results are then compared to the power spectra of the motions recorded at various points of an instrumented bridge (the base, the top of the pier, and the same location on the deck) from an actual earthquake. The method and results can explain many of the observed behavior very well although there are still some points that cannot be resolved due to lack of accurate input information and limitation of the method.

1. Introduction

Base isolation has been extensively used for bridges and buildings in the many countries worldwide, with excellent performances under strong ground motions. The application to bridges was a logical step, because bridges already have, in most cases, horizontal stiffness bearings located in between the desk and the piers that allow thermal expansion of the deck in the horizontal direction. The use of multi-layer elastomeric bearings for seismic protection was thus a natural extension of the rubber pads used for thermal expansion. A large number of studies have been conducted over the last a couple of decades to investigate the effectiveness of various types of isolation pads and the effect of their properties on the seismic response of bridges [1–7]. Recent research efforts include evaluation of hybrid isolation systems [8], comparison of performances of different isolation systems [9], performances of isolates structures subject to extreme seismic events [10], etc. In this paper, the application of base isolators to a real and specific structure, the Marga-Marga Bridge, near Viña del Mar, in the central coastal region of Chile, is evaluated. The effect of pile foundations and surface mat foundations underneath the piers (effect of soil structure interaction) on the shift of the natural frequencies of the structure and the change of dynamic amplification factors over the frequency range of interest, is considered and evaluated in this research as well. The bridge, built in 1996, was instrumented with 21 accelerometers distributed over the deck, along one pier, and in the free field. A number of earthquakes have been recorded by these instruments, including one happened on Feb 27, 2010, with a magnitude of 8.8, peak ground acceleration in the free field of about 0.35 g in the longitudinal direction of the bridge, over 0.34 g in the transverse direction and about 0.26 g vertically. The existence of these data and results of ambient vibration tests conducted immediately after completion of the construction provide a unique opportunity to evaluate the accuracy of different analytical models of the structure and our capacity to predict the observed behavior. This research is based on a new structural model, therefore provided a different perspective as a continuing effort interpreting the seismic behavior of the bridge.

* Corresponding author.
E-mail addresses: wentao.dai@hotmail.com (W. Dai), frojas@ing.uchile.cl (F. Rojas), shichen2004@hotmail.com (C. Shi), tanyong21th@tongji.edu.cn (Y. Tan).

https://doi.org/10.1016/j.soildyn.2018.07.024
Received 16 November 2016; Received in revised form 27 February 2018; Accepted 15 July 2018
Available online 30 July 2018
0267-7261/

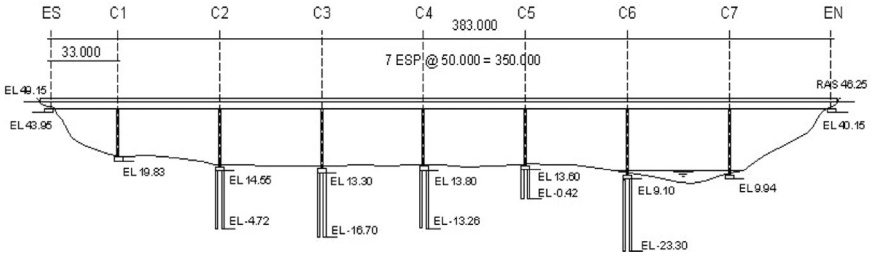

Fig. 1. Structural overview of Marga-Marga Bridge.

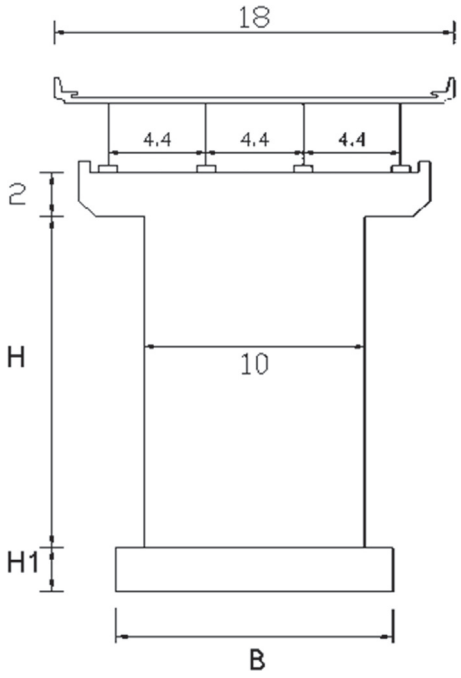

Pier #	H (m)	H1 (m)	B (m)
1	21.865	1.5	10.5
2	26.317	2.0	13.5
3	27.138	2.0	13.5
4	26.260	2.0	13.5
5	26.082	2.0	13.5
6	30.154	2.0	13.5
7	30.086	1.5	10.5

Fig. 2. Transverse view of pier and its dimensions.

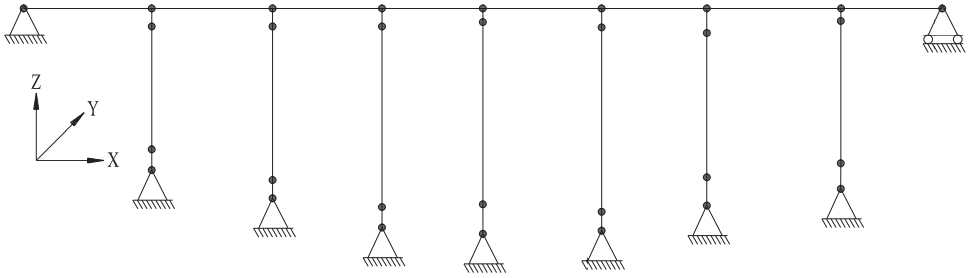

Fig. 3. Structural Model (without rubber pads).

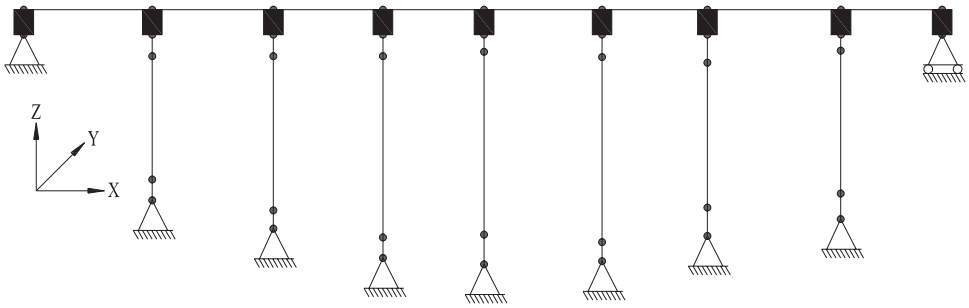

Fig. 4. Structural Model (with rubber pads, free deck).

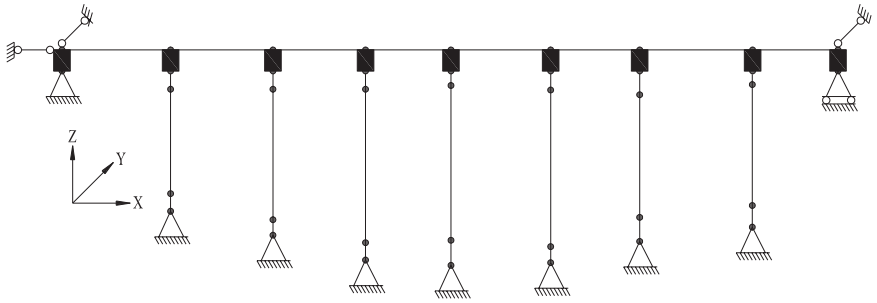

Fig. 5. Structural Model (with rubber pads, constrained deck).

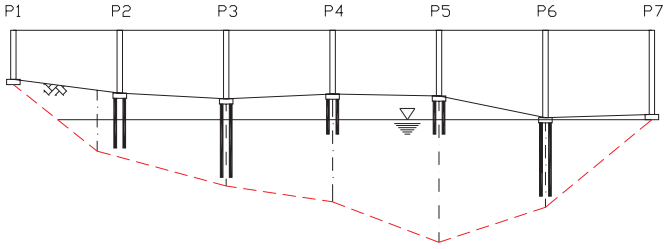

Fig. 6. Piers and pile groups of Marga-Marga bridge.

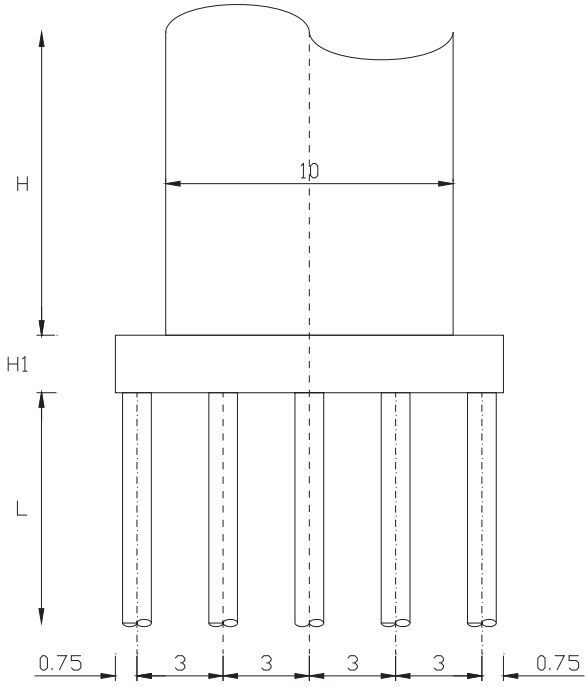

Fig. 7. A pier and its pile foundation.

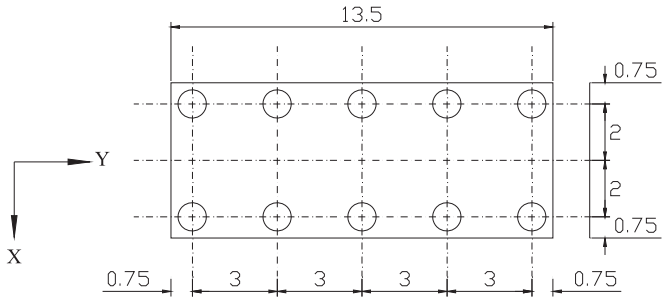

Fig. 8. Dimensions of cap and pile spacing.

Table 1
Dimension of the pier and cap.

Pier #	H (m)	H1 (m)	Width of Cap (m)
1	21.865	1.5	10.5
2	26.317	2.0	13.5
3	27.138	2.0	13.5
4	26.260	2.0	13.5
5	26.082	2.0	13.5
6	30.154	2.0	13.5
7	30.086	1.5	10.5

Table 2
Length and diameter of piles.

Pier #	L (m)	Diameter (m)
2	19.50	1.0
3	30.00	1.0
4	15.06	1.0
5	14.02	1.0
6	31.70	1.0

Results obtained in this research show that a free deck model can reproduce experiment results well longitudinally, while in the transverse direction a constrained deck is more realistic. It also can be concluded from this research that soil structure interaction effect is more significant in the transverse direction, probably due to its larger bending stiffness. Future research directions were suggested at the end of the paper.

2. Structural model and properties

A structural overview of the Marga-Marga bridge is shown in Fig. 1. The deck has a total length of 383 m and consists of 8 spans, all 50 m long except for the span connecting the north abutment and pier 1, which is 33 m long. The deck is a composite structure with a concrete slab on top of 4 structural steel wide flanges (I-beams). In the analysis program, the deck was modeled as an equivalent beam with an equivalent mass density, Poisson's ratio and Young's modulus of 2940 kg/m^3, 0.245 and 3.3×10^{10} Pa, respectively. The centroid of the equivalent beam cross section is 2.65 m above the top of the base isolators (rubber pads) and 0.45 m below the upper surface. The section properties of the equivalent composite deck are:

$$\begin{cases} A = 8.13(\text{m}^2),\ A_{sy} = 3.85(\text{m}^2),\ A_{sz} = 2.25(\text{m}^2) \\ I_z = 238.6(\text{m}^4),\ I_y = 5.98(\text{m}^4),\ J = 0.116(\text{m}^4) \end{cases}$$

in which A is the equivalent area of the deck's composite cross section; A_{sy} and A_{sz} are the effective shear areas of the composite cross section in the Y (transverse) and Z (vertical) direction, respectively; I_z and I_y are the bending moments of inertia in the Z and Y direction, respectively, and J is the torsional moment of inertia.

The piers and their dimensions are illustrated in Fig. 2. The

Table 3
Soil properties.

Layer	Pier 2		Pier 3 & 4		Pier 5		Pier 6	
	Thickkness (m)	Shear Wave Velocity (m/s)	Thickkness (m)	Shear Wave Velocity (m/s)	Thickkness (m)	Shear Wave Velocity (m/s)	Thickkness (m)	Shear Wave Velocity (m/s)
1	7.20	150.0	7.20	150.0	7.20	150.0	1.35	150.0
2	5.00	150.0	5.00	150.0	5.00	150.0	5.00	150.0
3	27.80	550.0	4.69	330.0	4.69	330.0	4.69	150.0
4	50.00	550.0	13.11	360.0	13.11	360.0	13.11	210.0
5			10.00	390.0	10.00	390.0	10.00	390.0
6			50.00	550.0	50.00	550.0	50.00	550.0

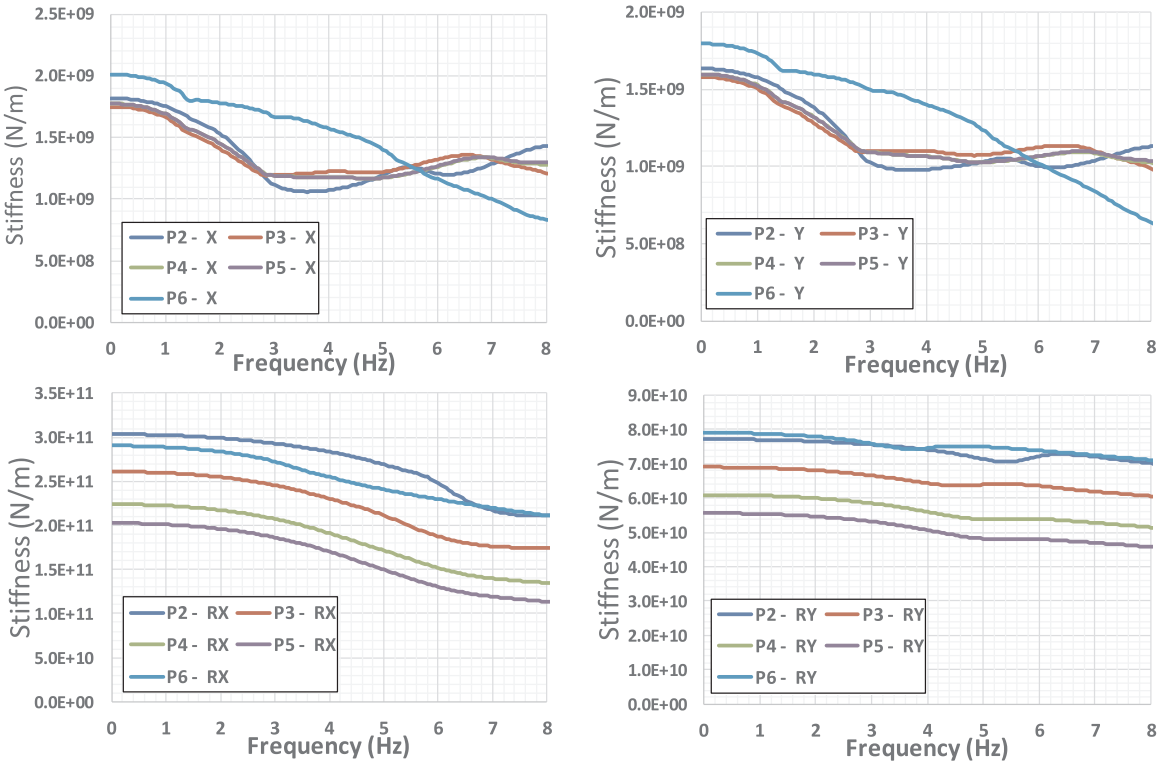

Fig. 9. Real parts of pile foundations stiffness.

formulation used in the present study, which will be discussed in the next chapter, assumes a constant cross section for each member (prismatic member). Each pier was therefore divided into three members according to the variation of the cross section. The top and bottom parts (members) are solid, while the long member in between is hollow. The mass density, Poisson's ratio and Young's modulus used in the analysis for the piers are 2500 kg/m^3, 0.2 and 3.3×10^{10} Pa, respectively. A material damping of 2% is assumed for all analyses in this study. The section properties of the piers are:

$$\begin{cases} A = 31.6(\text{m}^2),\ A_{sy} = 26.86(\text{m}^2) \\ I_x = 657.385(\text{m}^4),\ A_{sx} = 26.86(\text{m}^2) \\ I_y = 10.533(\text{m}^4),\ J = 37.92(\text{m}^4) \end{cases}$$

$$\text{and} \begin{cases} A = 6.38(\text{m}^2),\ A_{sy} = 4.17(\text{m}^2) \\ I_x = 63.33(\text{m}^4),\ A_{sx} = 1.25(\text{m}^2) \\ I_y = 4.18(\text{m}^4),\ J = 12.658(\text{m}^4) \end{cases}$$

for the top member and the middle member, respectively, while the section properties of the bottom members are:

$$\begin{cases} A = 74.25(\text{m}^2),\ A_{sy} = 63.113(\text{m}^2) \\ I_x = 1127.672(\text{m}^4),\ A_{sx} = 63.113(\text{m}^2) \\ I_y = 187.172(\text{m}^4),\ J = 552.531(\text{m}^4) \end{cases}$$

$$\text{and} \begin{cases} A = 57.75(\text{m}^2),\ A_{sy} = 49.088(\text{m}^2) \\ I_x = 530.578(\text{m}^4),\ A_{sx} = 49.088(\text{m}^2) \\ I_y = 145.578(\text{m}^4),\ J = 396.555(\text{m}^4) \end{cases}$$

for piers 2–6 and piers 1 & 7, respectively, where A_{sx} is the shear area in the X (longitudinal) direction and I_x is the bending moment of inertia around the X axis.

The rubber pads in the structure act as base isolators to mitigate the motions of the deck due to earthquakes. On the top of each pier, four rubber pads (each under one of the four steel wide flanges) were placed in a line, separately, along the transverse direction of the bridge. They were combined into one structural member in the analysis.

Rubber is a non-linear material, so the shear modulus of the rubber pads actually depends on the magnitude of the deformation. Daza [12] suggested a variation of the shear modulus with shear strain given by $G = 6.0 \times 10^5 \cdot \gamma^{-0.3764}$, while Moroni [13] suggested another relationship based on a series of test $G = 3.0 \times 10^5 \cdot \gamma^{-0.335}$. The length of the rubber pad members is 0.2 m, the mass density is 3000 kg/m^3 and material

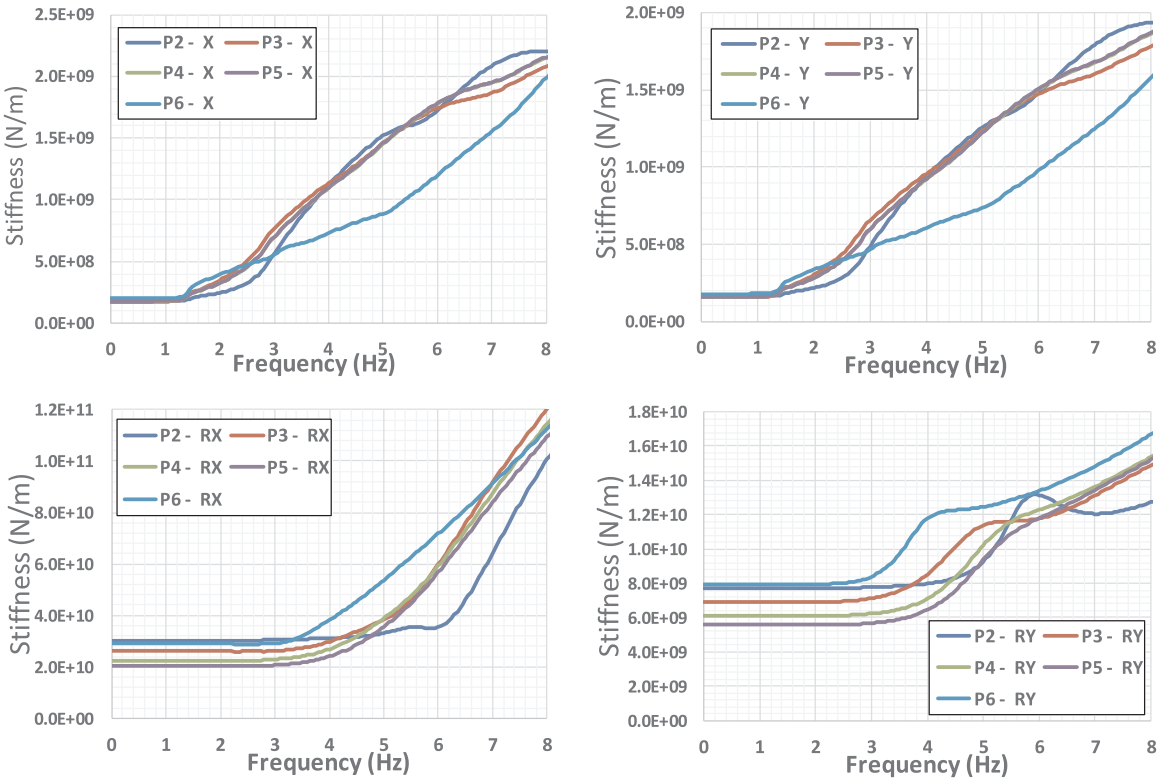

Fig. 10. Imaginary parts of pile foundations stiffness.

damping of 2% is assumed for this research. The cross section of each rubber pad is 0.85 by 0.55 m on top of the piers, 0.5 by 0.7 m at north abutment and 0.5 by 0.5 m at south abutment. The cross section properties of the rubber pad members used in the analysis are summarized as:

$$\begin{cases} A = 1.738(\mathrm{m}^2) \\ A_{sy} = 1.477(\mathrm{m}^2) \\ I_x = 168.269(\mathrm{m}^4) \\ A_{sx} = 1.477(\mathrm{m}^2) \\ I_y = 0.099(\mathrm{m}^4) \\ J = 35.845(\mathrm{m}^4) \end{cases}, \begin{cases} A = 0.906(\mathrm{m}^2) \\ A_{sy} = 0.770(\mathrm{m}^2) \\ I_x = 87.747(\mathrm{m}^4) \\ A_{sx} = 0.770(\mathrm{m}^2) \\ I_y = 0.017(\mathrm{m}^4) \\ J = 18.672(\mathrm{m}^4) \end{cases} \text{ and } \begin{cases} A = 1.109(\mathrm{m}^2) \\ A_{sy} = 0.943(\mathrm{m}^2) \\ I_x = 107.387(\mathrm{m}^4) \\ A_{sx} = 0.943(\mathrm{m}^2) \\ I_y = 0.037(\mathrm{m}^4) \\ J = 22.856(\mathrm{m}^4) \end{cases}$$

for rubber pads on top of the piers, at the north abutment and at the south abutment, respectively. The models used in this work are shown in Fig. 3(a model without isolation pads), Fig. 4 (an isolated model with a free deck) and Fig. 5 (an isolated model with a constrained deck). In the constrained deck model the deck is constrained in both X and Y directions at the left end (south abutment) and only in the Y direction at the right end (north abutment).

3. Structural formulation

In this work the analyses were conducted in the frequency domain determining the transfer functions for the motions (accelerations, velocities or displacements), the power spectra and their amplification factors at various points (locations of the recording instruments) due to a unit harmonic motion at the base of the foundation under all piers. An assumption has been made that the motions at the bases of all the foundations are the same, and is the same as that at the outcrop of the rock. Power spectra at locations of interests (top of pier and the deck) are constructed based on the transfer functions & power spectra at the rock outcrop, and are compared with those measured ones. The peaks of the transfer functions correspond to the natural frequencies of the system but only for those modes that will be excited when all supports move in phase. The transfer functions select therefore the significant modes from the point of view of the response to an earthquake with the same motion at all supports.

The model of the bridge used to obtain the transfer functions is a three dimensional frame model with continuous distribution of masses (by opposition to concentrated or consistent masses). The dynamic stiffness matrices in the frequency domain for linear structural members with continuously distributed masses were first used by Latona [14] to validate the accuracy of lumped and consistent mass matrices. Formulations for beam members and shell elements were then studied by many researchers. The structural formulation used in this research is very similar to the one formulated in Dai et al. [15] and Dai et al. [18], which implemented a complete three dimensional formulation for the most general dynamic case in the frequency domain with the consideration of continuous mass distribution, shear deformation, rotational inertia and, especially, axial load.

4. Dynamic stiffness of foundations

The Marga-Marga bridge, shown schematically in Fig. 6, has seven piers (P1–P7), five of them (P2–P6) with pile foundations. Each of the pile foundations consists of a 5 by 2 pile group (rows of 5 piles in the transverse direction of the bridge and 2 in the longitudinal direction), as shown in Fig. 7 and Fig. 8. Piers P1 and P7 have surface mat foundations without any supporting piles.

To calculate the stiffness of these pile groups, the interaction between two different pile groups is neglected, assuming each pile group embedded in a horizontal layered soil deposit extending to infinity in the two horizontal directions, based on the fact that the distance between pile groups is much larger than the horizontal dimension of the pile groups themselves. The dimensions of the piers and their pile foundations are illustrated in Table 1 and Table 2.

The soil properties under each pier, including the thickness of each layer and its shear wave velocity, are shown in Table 3. The soil deeper than 40 m is assumed to have a high shear wave velocity of 550 m/s

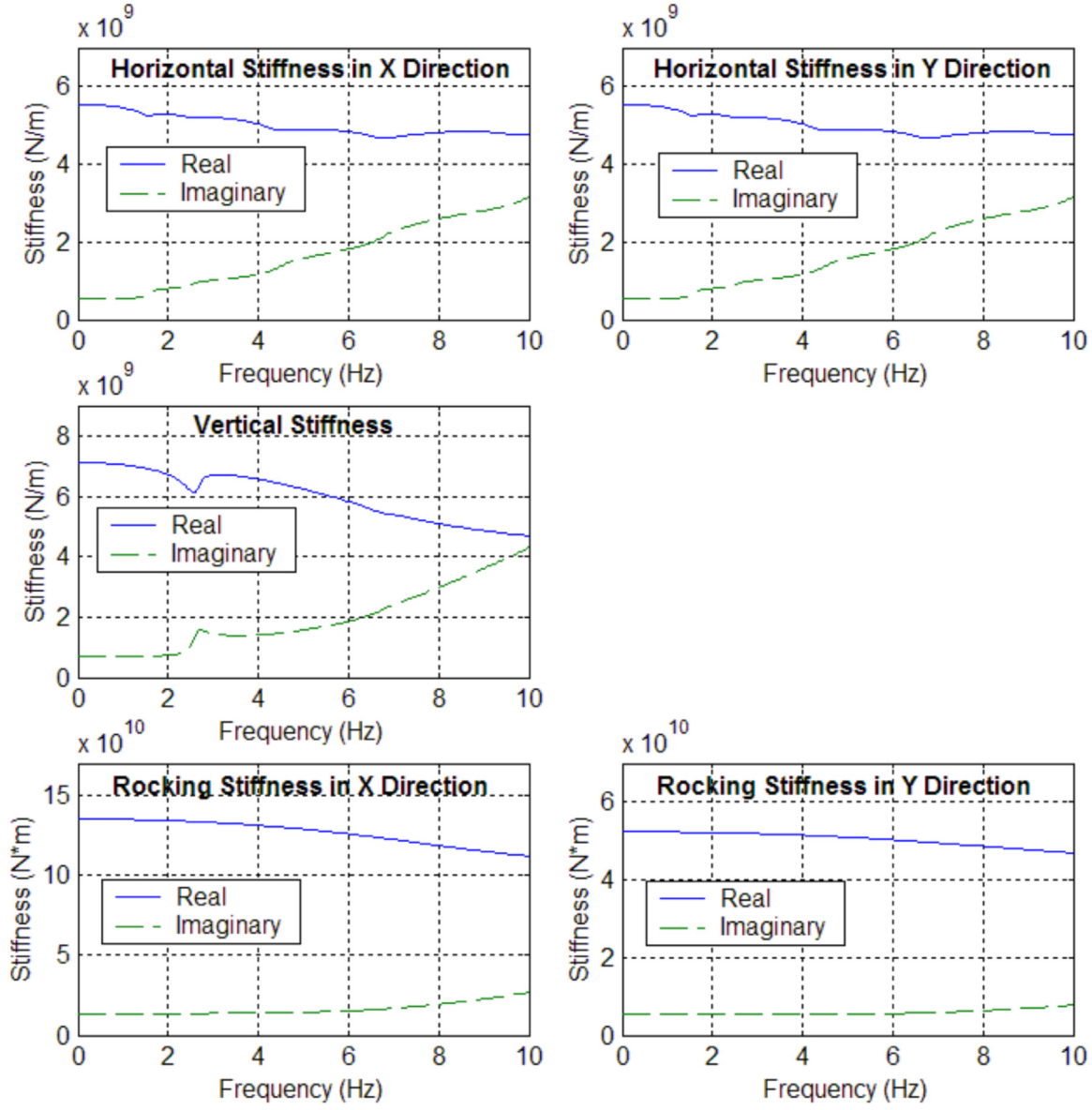

Fig. 11. Surface mat foundation stiffness under Pier 1 & 7.

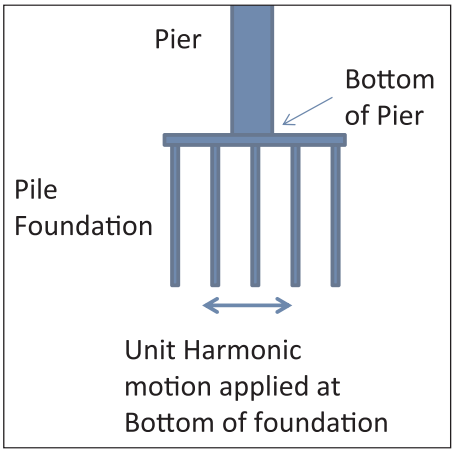

Fig. 12. Pier and pile foundation system.

because their effect on pile foundation stiffness is very high, while the layers shallower than 40 m have shear wave velocities in the range of 150–400 m/s per test results. All the soils are assumed to have a Poisson's ratio and internal damping of 0.25% and 5%, respectively, and a mass density of 2000 kg/m^3 is adopted in the analysis also based on test results. The piles are made of concrete with a Young's modulus of about 3×10^{10} Pa. The mass density and internal damping are assumed to be 2500 kg/m^3 and 5%, respectively. This represents an E_p/E_s ratio (ratio of Young's modulus of pile over that of soil) of 75–100, indicating a stiffer soil than the one normally encountered with pile foundations.

In this study, a formulation which employs an analytical solution in the frequency domain in the horizontal directions and a numerical discretization vertically is adopted. This eliminates the need of a non-reflecting boundary in the horizontal direction. The details of the methodology to calculate the dynamic stiffness of the pile foundations and surface mats can be found in Dai and Roësset [17] and Dai [16]. Dai et al. [19] shows the comparison of the calculated pipe foundation stiffness to some experimental data. The calculated foundation stiffness can be found in Fig. 9, Fig. 10 and Fig. 11. It can be seen that the real part of the horizontal stiffness reduces with frequency like a parabolic curve for low frequency ranges and has a dip at about 1.4–1.6 Hz,

Table 4
Natural frequencies of Marga-Marga bridge from previous studies (Hz).

		Longitudinal				Transverse				Vertical		
Experimental Data 1 (May 1996)		1.86				1.17	1.42	2.1				
Experimental Data 2 (July 1996)		1.71				1.07	1.27	1.9				
M.E. Segovia (1997)	**No Rubber Pads**	3.85				2	2.22	2.7				
	5% Deformation	1.54				0.71	1.02	1.85				
D. Romo (1999)	**No Rubber Pads**	2.01	2.13	2.39	2.77	1.29	1.79	2.67	3.36			
	Free Deck	0.65	2.09	2.24		0.93	2.18		1.87			
	Constrained Deck	2.01	2.03	2.1	2.25	0.93	1.28	2.18				
V.M. Daza (2003)		0.67	2.5	2.8		0.96	1.5		1.88	2.1	2.56	

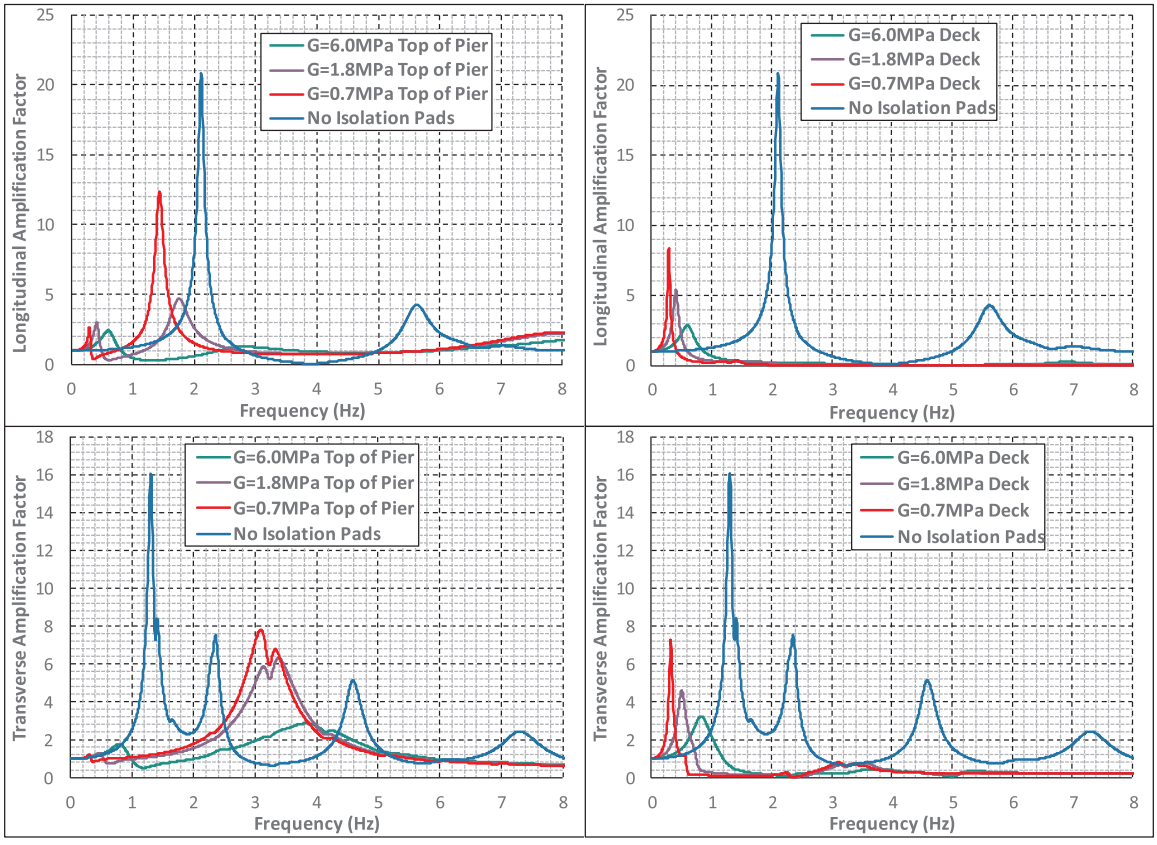

Fig. 13. Transfer functions at top of pier and deck with a free deck.

which corresponds to the fundamental natural frequency of the soil deposit.

5. Results

5.1. Longitudinal direction

Fig. 13 & Fig. 14 show the transfer functions of the motions on top of pier 4 (center pier) and deck over pier 4 due to a unit harmonic motion at the bottom of all foundations (including south and north abutment), as shown in Fig. 12, with the assumption that all foundation bottom motions are in phase.

It can be seen that, in the longitudinal direction (at the top of the figures), without rubber pads, the two most significant peaks of the transfer function due to the same unit harmonic base motion at all piers occur at 2.15 Hz and 5.6 Hz, respectively. The first peak occurs at a frequency very similar to that of the first two modes reported by Romo [11] (2.01 Hz and 2.13 Hz) for the same case, as shown in Table 4.

The isolation pads (rubber pads) will change the frequency response characteristics of the structure significantly. Results with equivalent shear modulus of the isolation pads of 6.0 MPa, 1.8 MPa & 0.7 MPa, are shown in Fig. 13 & Fig. 14, which correspond to a shear deformation of 0.22%, 5.4% & 66%, and an equivalent damping ratio of 28%, 14% & 8%, according to the result of a regression analysis of experimental data reported by Moroni [13] and Daza [12], respectively. It can be seen that the frequencies at the first two significant peaks have been reduced to 0.3–0.65 Hz and 1.4–1.8 Hz for the top of pier 4 with a free deck (this peak is not very significant with 6.0 MPa isolation pads shear modulus because of high damping ratio), while a peak at about 0.3–0.65 Hz for the deck over pier 4, depending on the values of isolation pads shear modulus. With a constrained deck, there is a peak at about 1.4–1.8 Hz for the motions at the top of pier 4, and peaks at 1.6–1.8 Hz & 6.4–6.6 Hz for the deck. It should be noted that the amplitude of the first peak at the deck over pier 4 is larger than that on top of the pier for a free deck. In other words, the motion at the deck has been amplified from the top of the pier at this peak if a free deck is assumed. The first peak for a free deck (0.3–0.65 Hz) agrees with Romo [11] (0.65 Hz), whose research assumes an equivalent shear moduls of 6.0 MPa as shown in Table 4, while the peak at 1.4–1.8 Hz are in good agreement with both Ambient tests (1.86 and 1.71 Hz) and Romo's results

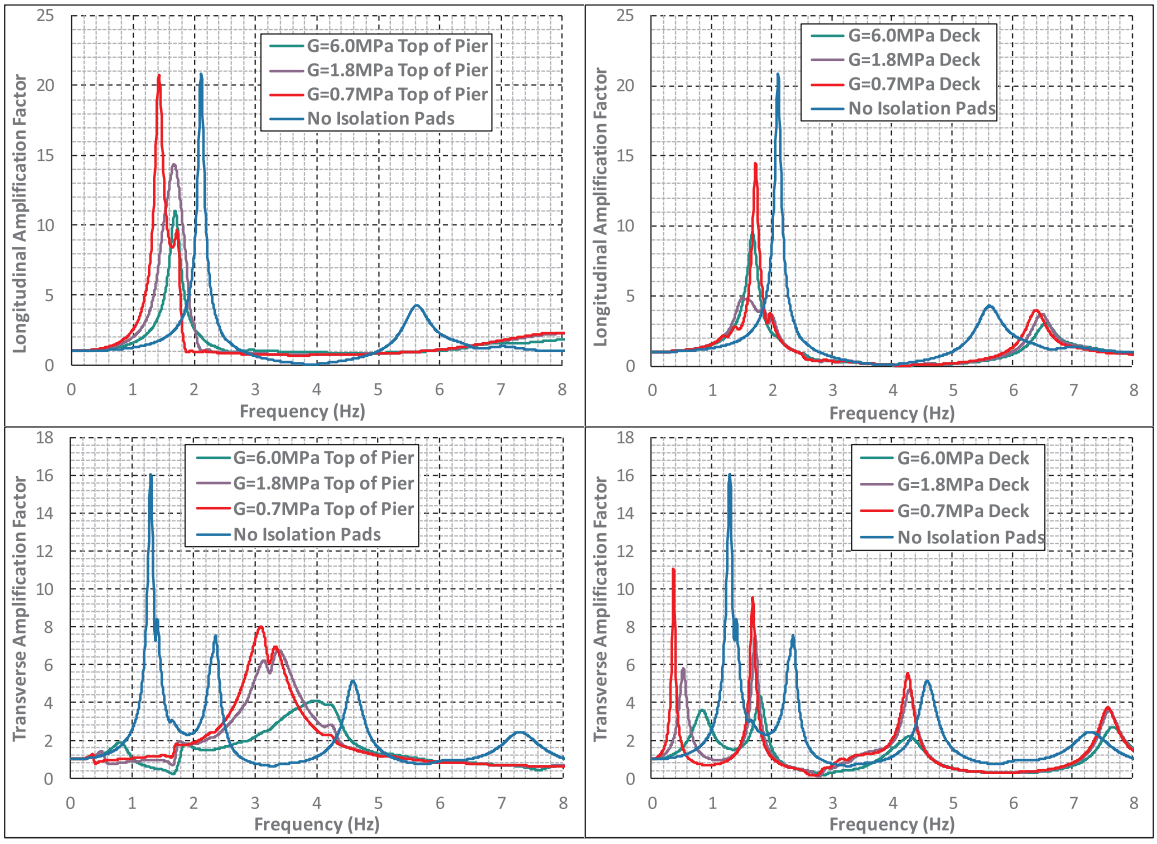

Fig. 14. Transfer functions at top of pier and deck with a constrained deck.

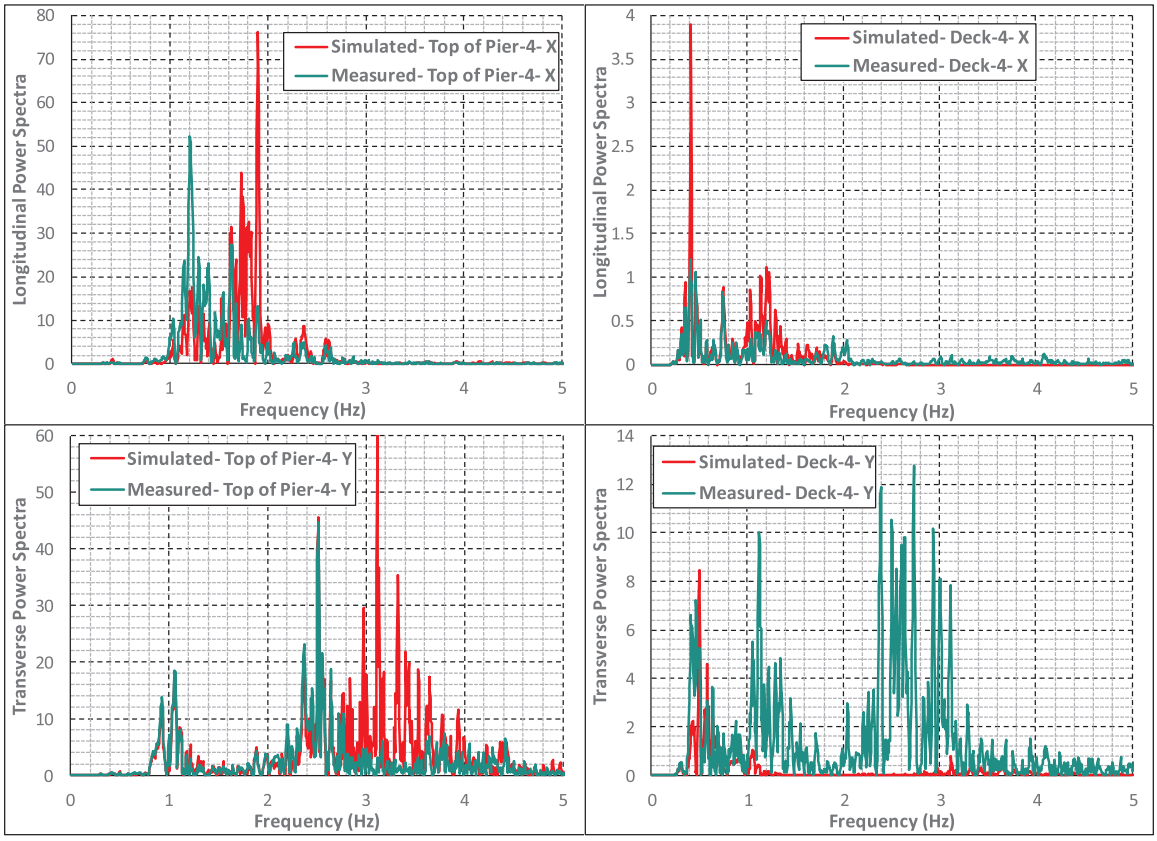

Fig. 15. Comparison to measured data with an equivalent G = 1.8 MPa and a free deck.

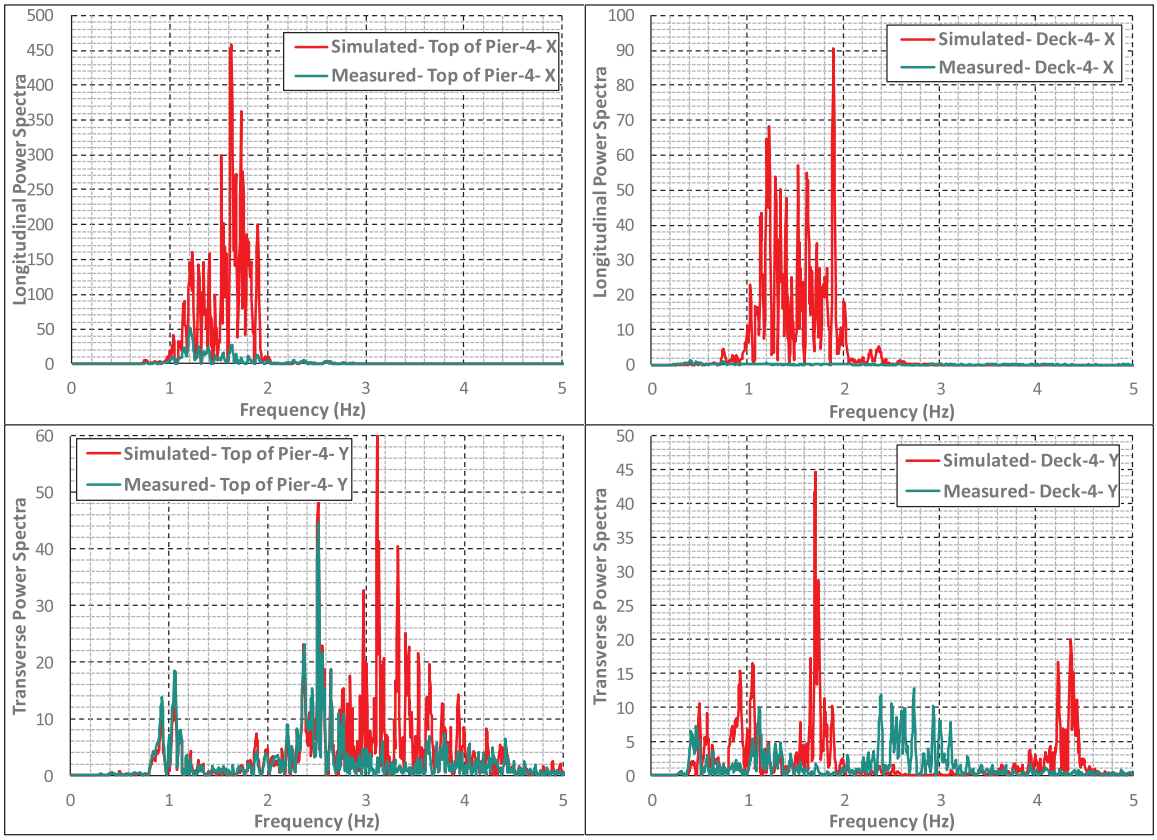

Fig. 16. Comparison to measured data with an equivalent G = 1.8 MPa and a constrained deck.

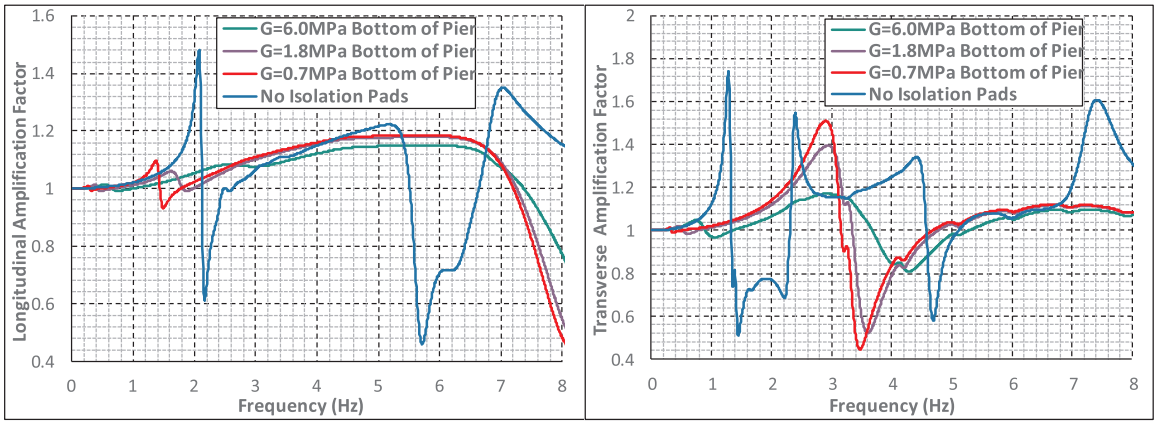

Fig. 17. Transfer function at the bottom of pier with a free deck.

(2.0–2.1 Hz) for both a free and constrained deck.

5.2. Transverse direction

In the transverse direction, without rubber pads, the first three significant peaks are at 1.30 Hz, 2.35 Hz and 4.55 Hz, respectively, as shown in Fig. 13 & Fig. 14, again. There are also some less significant peaks at 1.40 Hz and 7.30 Hz due to motions at base of all piers. The frequency of the first peak is in very good agreement with D. Romo's results for the same case (1.29 Hz).

With isolation pads, for the motion at the top of pier 4, significant peaks are observed at frequencies of about 3.1–3.4 Hz for both a free and constrained deck. It can also be seen that peaks are at 0.35–0.9 Hz for the motions at the deck over pier 4 with a free deck, while more peaks can be observed around 0.35–0.9 Hz, 1.7–1.9 Hz, 4.3 Hz and 7.6–7.8 Hz with a constrained deck, for different combinations of equivalent shear modulus and equivalent damping ratio of the isolation pads. The first peak of the deck (0.35–0.9 Hz) agrees well with Romo's model (0.93 Hz) with a large shear modulus, as shown again in Table 4.

6. Comparison to experimental data

On Feb 27, 2010, an earthquake, with a magnitude of 8.8, hit Chile, and some experimental records were obtained through the instrumented bridge, Marga Marga Bridge, in central Chile. The measured power spectra at the top of pier 4 and at the deck were compared against the calculated ones from this study, as shown in Fig. 15 & Fig. 16.

Fig. 15 shows the comparison to the measured data with an equivalent shear modulus of 1.8 MPa for the isolation pads with a free

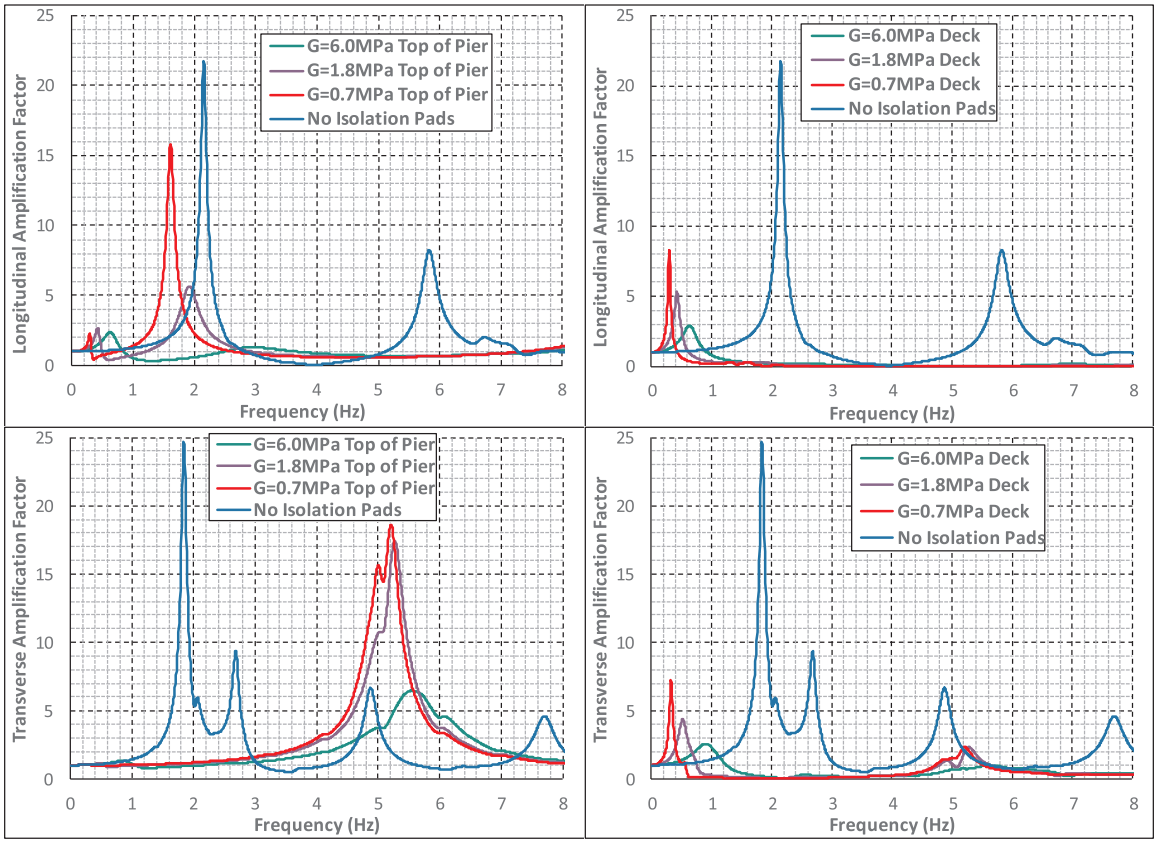

Fig. 18. Transfer functions at top of pier and deck with a free deck without consideration of soil structure interaction effect.

deck in the longitudinal (top part of the figure) and transverse direction (bottom part of the figure). It can be seen that, at the top of the pier, the simulated power spectra are in relative good agreement with the measured ones both longitudinally and transversely, and the amplitude over most of the frequencies can be reproduced without significant discrepancies except over 1.7–2.0 Hz in the longitudinal direction and 2.7–3.3 Hz in the transverse direction. In the longitudinal direction, the amplitude at about 1.2 Hz is under-estimated by the model used in this research by a factor of 3.0 (about 70% under estimation in terms of displacement or acceleration amplitude), while in the transverse direction the model and methodology used in this study can reproduce the measured power spectra very well for the frequencies below 2.7 Hz.

At the deck, on the contrary, the power spectra were over-estimated in the longitudinal direction at two peaks (0.4 Hz and 1.2 Hz) by a factor of 2–3 (40–70% over estimation in terms of displacement or acceleration amplitude), while in the transverse direction the analysis can only reproduce the power spectra amplitude at very low frequencies and under-estimate over the rest of the frequencies by a large margin, as shown in the lower right part of Fig. 15. The amplification ratio, of course, is a function of damping ratio of structure members.

With a constrained deck, it can be seen that the model will over-estimate the power spectra amplitude by a very large margin in the longitudinal direction at both top of the pier & deck, as shown in the top part of Fig. 16. In the transverse direction, the simulated spectra are very similar to that with a free deck at the top of pier (lower left of Fig. 16), while at the deck the simulated spectra are not very successful (lower right of Fig. 16).

To sum up, comparison between the measured and simulated power spectra indicates that:

1) The simulated power spectra in general are in good agreement with the measured ones. In the longitudinal direction, a free deck is more realistic, but the real boundary conditions longitudinally at the two ends of the deck (two abutments) should be more complicated and require extended research.
2) In the transverse direction, the motions at the top of pier can be very well reproduced and are not affected by the deck boundary conditions, while at the deck, it looks like a constrained deck is more realistic although the measured spectra were poorly reproduced by both models.
3) One of the limitations of the frequency domain analysis is the assumption of the same shear modulus for all isolation pads, however in reality different isolation pads may have different shear strain levels, therefore different shear module and equivalent internal damping ratios, especially in the transverse direction.
4) Spatial attenuation effect in the soil deposits should be considered and simulated to estimate the phase differences of the motions at the bases of the pile foundations to improve the results.

7. Effect of soil structure interaction

Fig. 17 shows transfer functions at the bottom of pier 4 with a free deck due to a unit harmonic motion at the bottom of all foundations for various shear module of the isolation pads. If no soil structure interaction is considered (or a rigid foundation) in the analysis, the unit harmonic motion will be applied at the bottom of all piers and transfer functions shown in Fig. 17 will be a constant value of 1.0 for all frequencies. The variation of these transfer functions indicates the effect of soil structure interaction. It can be seen that in general a structure without isolation pads shows more soil structure interaction effect because of its overall higher stiffness than an isolated one. For a base isolated structure, in the longitudinal direction, the transfer functions at the bottom of pier gradually increase from 1.0 to about 1.2 at about 6.5 Hz and then reduce sharply to about 0.4 at about 8.0 Hz, which indicates that the soil structure interaction effect below 7 Hz is not significant. However, the effect of soil structure interaction is more

significant in the transverse direction. The transfer functions increase to about 1.5 at about 3.0 Hz, then drop sharply to about 0.4, gradually come back to 1.0 at about 6.0 Hz and become stable, which indicates a natural frequency of the system at about 3.2 Hz in the transverse direction, as shown in Fig. 17.

Fig. 18 shows the same information as Fig. 13, but without the consideration of soil structure interaction effect. When comparing the two figures, one can conclude that, for a structure without isolation pads, soil structure interaction has very little effect in the longitudinal direction. The first peak at 2.1 Hz does not change, while the second peak at 5.8 Hz shifts slightly to 5.6 Hz. In the transverse direction, the soil structure interaction effect is more prominent, and the first three peaks at 1.8 Hz, 2.7 Hz and 4.9 Hz shift to 1.3 Hz, 2.35 Hz and 4.6 Hz due to the effect of soil structure interaction, respectively.

When isolation pads are present, in the longitudinal direction, one can see that the shift of the peaks is very small and negligible. In the transverse direction, it can be seen that at the top of the pier the first peak shifts significantly from about 5.2 Hz to about 3.2 Hz, and amplification ratio reduces from about 17.0 to about 7.0 for the case with 1.8 MPa isolation pad shear modulus, while no significant change of the peaks can be observed at the deck.

To sum up, the soil structure interaction effect is more significant transversely than longitudinally, more at the top of pier than at the deck, which is consistent with the findings from Fig. 17. Soil structure interaction has its largest effect on the transverse motion at the top of pier, as shown in the lower left of Fig. 18. The rectangular shape piers used on this bridge are much stiffer, in terms of bending stiffness, in the transverse than longitudinal direction ($I_x \gg I_y$) as discussed in the structural properties, and it is well known that soil structure interaction has more effect on stiffer structures, which provide a reasonable explanation why soil structure interaction effect is more significant transversely.

8. Concluding remarks

Transfer functions and power spectra were calculated at various positions of an instrumented bridge through a frequency domain solution with the consideration of distributed mass and rotatory inertia. Soil structure interaction effect were considered using separately computed dynamic stiffness of pipe foundations. Results agree well with experiment results, especially in the longitudinal direction. Soil structure interaction effect is more important in the transverse direction than longitudinal, more on the deck than top of pier for an isolated structure.

It can also be concluded that, in order to obtained better agreement with experiment data, more details of input information must be considered in the analysis and more realistic modeling of rubber pads and pier base motions is desired.

References

[1] Turkington DH, Carr AJ, Cooke N, Moss PJ. Seismic design of bridges on lead rubber bearings. J Struct Eng 1989;115(12):3000–16.

[2] Chaudhary M. Evaluation of seismic performance of base isolated bridges based on earthquake records [Ph.D. Dissertation]. Japan: Department of Civil Engineering, University of Tokyo; 1999.

[3] Chaudhary MTA, Abe M, Fujino Y, Yoshida J. System identification of two base-isolated bridges using seismic records. J Struct Eng 2000;126(10):1187–95.

[4] Chaudhary MTA, Abe M, Fujino Y. Performance evaluation of base-isolated Yamage bridge with high damping rubber bearings using recorded seismic data. Eng Struct 2001;23(8):902–10.

[5] Jangid RS. Seismic response of isolated bridges. J Bridge Eng 2002;9(2):156–66.

[6] Boroschek R, Moroni M, Sarrazin M. Dynamic characteristics of a long span seismic isolated bridges. Eng Struct 2003;25:1479–90.

[7] Daza VM, Moroni M, Roesset JM, Sarrazin M. Seismic behavior of a bridge with base isolation. In: Proceedings of the 11th NSGCL, Memphis, USA.

[8] Cancellara D, De Angelis F. Nonlinear dynamic analysis for multi-storey RC structures with hybrid base isolation systems in presence of bi-directional ground motions. Compos Struct 2016;154:464–92.

[9] Cancellara D, De Angelis F. Assessment and dynamic nonlinear analysis of different base isolation systems for a multi-storey RC building irregular in plan. Comput Struct 2017;180:74–88.

[10] Cancellara D, De Angelis F. A base isolation system for structures subject to extreme seismic events characterized by anomalous values of intensity and frequency content. Compos Struct 2016;157:285–302.

[11] Romo D. Analisis de registros sismicos y microambientales en el Puente Marga-Marga. Santiago, Chile: Engineering Thesis Civil Engineering Department, University of Chile; 1999.

[12] Daza VM. Interaccion sismica suelo-estructura en el Puente Marga-Marga. Santiago, Chile: Engineering Thesis, Civil Engineering Department, University of Chile; 2003.

[13] Moroni MO. et al Analysis of seismic records obtained in isolated structures. In: Proceedings of the 12th World Conference on Earthquake Engineering, Auckland, New Zealand; 2000.

[14] Latona RW. Analysis of building frames for natural frequencies and natural mode shapes. Cambridge, Massachusetts: Inter American Program, Civil Engineering Department, MIT; 1969.

[15] Dai W, Yu CP, Roësset JM. Dynamic stiffness matrices for analyses in the frequency domain. Comput-Aided Civil Infrastruct Eng 2007;22(4):265–81.

[16] Dai W. Evaluation of base isolation and soil structure interaction effects on the seismic response of bridges [Ph.D. Dissertation]. College Station, TX.: Department of Civil Engineering, Texas A&M University; 2005.

[17] Dai W, Roësset JM. Horizontal dynamic stiffness of pile groups: approximate expressions. J Soil Dyn Earthq Eng 2010. https://doi.org/10.1016/j.soildyn.2009.12.010.

[18] Dai W, Moroni MO, Roësset JM, Sarrazin M. Effect of isolation pads and their stiffness on the dynamic characteristics of bridges. J Eng Struct 2006;28(9):1298–306.

[19] Dai W, et al. A numerical solution and evaluation of dynamic stiffness of pile groups and comparison to experimental results. J Eng Struct 2017;151:253–60.